International Journal on Artificial Intelligence Tools
Vol. 32, No. 3 (2023) 2340012 (29 pages)

DOI: 10.1142/S0218213023400122

Breast Masses Segmentation: A Framework of Skip Dilated Semantic Network and Machine Learning

Saliha Zahoor* and Umar Shoaib†
Computer Science Department, Hafiz Hayat Campus
University of Gujrat, Gujrat 50700, Pakistan
**saliha.zahoor@uog.edu.pk*
†umar.shoaib@uog.edu.pk

Ikram Ullah Lali
Information Science Department, University of Education
Lahore, 54000, Punjab, Pakistan
m.i.lali@ue.edu.pk

Received 19 January 2022
Accepted 22 September 2022
Published

Many medical specialists used Computer Aided Diagnostic (CAD) systems as a second opinion to detect breast masses. The poor visualization of mass images makes it difficult to identify precisely. To segment the lesions from the mammograms is a difficult task due to different shapes, sizes, and locations of the masses. The motivation of this study is to develop a method that can segment breast mass lesions from mammogram images. The objective is to perform the segmentation of the breast mass mammogram images more precisely at an early stage. Breast mass segmentation is always a basic requirement in computer-aided diagnosis systems. In this study segmentation of the masses abnormalities from the mammogram images is performed by using the Skipping Dilated semantic segmentation approach. The study uses class weights and Dilation factor using semantic Convolutional Neural Network (CNN). It overcomes the class misbalance in tumors and background class, that affect the mean Intersection over Union (MIOU), and weighted-IOU (WIOU) by using class weights. Secondly, dilation convolution magnifies the receptive field exposure that enriches the convolutional operation with context attentiveness. Two public datasets of mammography INbreast and CBIS-DDSM are used. The WIOU of Skipping Dilated Semantic CNN for INbreast is 98.95% and CBIS-DDSM is 94.82% achieved.

Keywords: Deep learning; layers; mammograms; masses; segmentation; weights.

1. Introduction

The second-leading cause of death globally is breast cancer. However, detecting breast masses in an early stage can reduce the mortality rates. Breast cancer affects many women around the world. The tumor arises in the lining of ducts and lobules of the breast due to the irregularity of the cells. According to the global cancer statistics report, 684 996 deaths were reported globally, and 2261 419 women were detected with breast cancer.[1] Early detection is required to reduce the death rate. Mammography tests perform the early screening diagnosis. The early diagnosis can minimize the death rate and can increase treatment of recovery. Mammography test is low energy dose recommended test at an initial stage to detect cancer. The investigation of mammogram images always remains a challenge for researchers. Radiologists examine the abnormality and determine the location and shape of suspicious breast regions. More accuracy and precision are required for the process. The errors can be originated due to number of mammography tests. To help the radiologists many CAD systems have been developed. The CAD systems help the radiologists to detect and segment the tumors with the lowest errors in mammography. However, due to irregular shapes and poor contrast this is a stimulating to segment the tumor.[2]

It is not easy to examine the hundreds of images daily and detect the correct result. This procedure for the radiologist is time-consuming and generates more false-negative results due to the manual process. More than one radiologist's opinions are added to most labs to diagnose the tumor. The radiologists usually use computer-aided diagnosis (CAD) systems as supporting tools for making a final opinion. CAD is essential for reducing false results while preserving information and support as a second reader to the radiologist.[3]

There have been numerous CAD systems created, but they have a false detection rate, due to various sizes, shapes, low contrast, noises ratio in the masses' visibility, masses locations, and presence of pectoral muscles. These automated systems should be improved.[4] The low accessibility of the marked dataset obstructs the progress and assessment of CAD systems. Mostly CAD system mass detection rate is below 90%. Masses detection is difficult due to its similarity with the breast's other parts. To detect and segment the masses the lot of preprocessing is required.[5] Many suggested CAD systems have slow run times and memory difficulties because of the appearance, shapes, and placements of the masses. The majority of segmentation techniques are nebulous and unsuccessful.[6] There are numerous existing methods for segmenting the masses. These systems performance of masses segmentation is not very good. Images patches can be extracted manually or automatically. Systems that are semi-automated are being suggested. Manual mass extraction requires effort and lacks in accuracy. In Ref. 7, Sun *et al*. describe that the masses segmentation automatically in the form of patches also imprecise due to errors. Several studies have been conducted to detect the position of the masses. However, most of them are not focused on mass segmentation. Most studies performed just detection of masses.[8] Some studies have focused on patch-based strategies using the Mask-RCNN approach.[9] The images are resized using 512∗512 and converted into the PNG format. The masses have been identified using the Mask-RCNN method.[10] To facilitate the deep neural network training and testing, the resizing in image preprocessing is required step. The patch extraction method reduces the network's field of view. Patch correlations must be carefully constructed to increase the accuracy. The image resizing provides sufficient information for the segmentation procedure to proceed. After resizing the mammography images, the attention UNET is employed to segment the masses.[7]

The large-scale images are segmented using deep learning techniques. Deep learning technologies are used to segment the masses more precisely and accurately by replacing conventional thresholding methods and lowering the false-positive rates. The human intervention and semi-automated work has been reduced by the deep learning. The best dilation convolution usage prevents the loss of resolution and coverage because it supports exponential expansion. It allows the large perceptive without increasing the parameters based on memory and computation costs. It also preserves the resolution of the images. Most researchers used traditional CNN models that consume much computing resources.[11]

To perform the segmentation of the masses mammogram images proposed a new framework by using skipping dilated semantic segmentation network. The skipping dilated semantic segmentation is more promising method. The kernels are enlarged by inserting holes between the kernel elements by using dilated convolution that is a type of convolution. It is a more popular method for image segmentation because it expands the image size by increasing the dilation rate. To improve the neural network's performance and convergence the skip adds the output of one layer as an input to the next layers.

The publically available dataset INbreast[12] and CBIS-DDSM (Curated Breast Imaging Subset of Digital Database for Screening Mammography) that is a modernized form of DDSM[13] used for segmentation.

The CBIS-DDSM dataset has high contrast as compared to the INbreast dataset.[7] Many studies perform data augmentation and use ROI patches of the CBIS-DDSM images.[10] Segmentation of the small mass lesions from the mammogram images is challenging and uncertain.[14] The authors resized the mammogram images into $256*256$ but could not find the small mass from the high density image.[15] The resizing of the mammogram images is performed into $512*512$ to detect the small and large masses from the images.[7,15]

In this study, 1592 CBIS-DDSM and 107 INbreast dataset mass images are used for segmentation process. Image preprocessing is required to adjust the size using the patch or resizing method. In image patch extraction procedure there is chance to eliminate the useful information so resizing of the images approach used. The images are resized to ensure that they are all the same size. Images with a resolution of $512*512$ are used. The resizing of the images is performed by applying interpolation method.

The preprocessing of the whole mammogram images is performed. The noise is removed from the images. The improvement and sharpens of the images are performed. The enhancement of the images is performed by using the CLAHE method. The mammogram images are low contrast and low-resolution images so enhancement is performed to increase the visibility of the images.

After preprocessing phase, the segmentation of the images is performed to predict the abnormality region. The abnormality region is detected using the deep learning model approach. The proposed approach is skipping dilated semantic CNN. The other model semantic CNN without skipping dilated approach is also applied on the dataset just to verify the effect of the model. Many researchers used the CNN model for segmentation. Segmentation is used to identify the more precise abnormal region of interest (ROI) and to analyses the more vital aspects of the breast. The segmentation process extracts meaningful information. The purpose of semantic segmentation without dilation factor and skip connection is just to check the precision and accuracy. The results of semantics segmentation are compared to the proposed skipping dilated semantic convolution model. The proposed skipping dilated convolutional kernels replace the traditional CNN kernels. The proposed method by using skipping dilation is much better than a convolutional model without a dilation factor.

The purpose of these two models is to check the precision and accuracy of the segmentation results. The recommended method performed the automated segmentation by eliminating the unnecessary parts like pectoral muscle from the breast region. Post-processing is performed after predicting the abnormal region to clear the results by using morphological operations. The proposed segmentation results well mapped the ground truth of the dataset. The proposed model performed the best results for the segmentation. Our proposed model can predict different types of lesions of different shapes, sizes, and locations. The model can predict the small ROI also. The accuracy of segmentation is measured by using the Dice Index (DI), mean IOU (MIOU), and weighted-IOU (WIOU). The 98.51% segmentation masses accuracy of the INbreast dataset is achieved. The proposed model proved that proposed results are better than the other recommended methods.

The proposed method's results show the 94.82% WIOU for masses segmentation of CBIS-DDSM. In this paper, skipping dilated semantic CNN method for breast mammogram images segmentation is proposed. The model was tested using two publicly available datasets. The consequences determine that the proposed CAD system has significantly improved masses segmentation. The removal of pectoral muscle is also performed by performing the segmentation of masses. The following are the main contributions of this research work:

- Proposed method automatically detects regions of interest and performs segmentation of masses by presenting a new framework model based on skipping dilated semantic CNN.
- Frequency-based weights of pixel-wise classes are assigned.
- The automated CAD system can detect the different shapes, sizes, and types of masses in different locations.
- The performance of semantic segmentation method is improved significantly by using the skipping and dilation factor to perform the segmentation of the breast mass mammogram images more precisely by eliminating the other organs of the breast.

The breakdown of the paper is systematized as second section describes the related work, the third section illustrates methodology, the fourth section consists of results and experiments, the fifth section provides the discussions, and the sixth section discusses the future work.

2. Related Work

There are many image preprocessing and segmentation methods proposed by the other researchers. In the preprocessing field, the noise, blur from the images are removed to increase the sharpness of the images. Many effective methods have been proposed to enhance the mammogram images for CAD and manual patch extraction. The noise is also removed from the images by increasing the contrast enhancement of the images.[16] The preprocessing is performed to increase the image's contrast, enhance the mammogram's boundaries, edges, and detect the suspicious regions.[17] Various preprocessing methods have improved the image's brightness, reduced noise, and remove artifacts and labels. CLAHE and morphological operations are examples of preprocessing techniques. In these techniques, image noise is reduced using median, average, max, and min filters. Power law, logarithmic, and top hat operations are used as transformation methods.[18,19] Contrast enhancement methods can sometimes outperform system improvements. There should be a way to control image enhancement in the histogram techniques. The CLAHE method has been used to alleviate this problem and adjust the enhancement limit in mammogram images without sacrificing vital information.[20,21] Homomorphic filtering techniques and modified histogram contrast enhancement are presented.[22] The mean filter can reduce the edge information, so mean filters with the wavelet transform methods are used to enhance the images without losing any information.[23]

After preprocessing phase, the second phase is segmentation. Some CAD systems do not perform segmentation; they only perform the classification based on images ROI extracted patches. These systems have high speed and simple processing techniques. These CAD systems have a simple structure.[24] The suspicious mass region extracted from the mammograms in the segmentation phase. Different CAD systems have been proposed for mass segmentation. Most CAD systems for mammography images are proposed based on machine learning methods. The CAD systems are developed to help the radiologist effectively to detect, diagnose and classify the abnormality from the images. CAD systems are developed to reduce the false-positive rates in different medical imaging fields. These CAD systems used manual cropping, thresholding, region growing, supervised, and unsupervised methods for masses segmentation.[25] Clustering methods like K-means and active contour have been used for breast images segmentation.[26] The discrete dynamic contour techniques are used to segment the breast tumor.[27] To perform masses segmentation an adaptive region growing algorithm is proposed.[28] The mass segmentation is performed using the deep fully convolution net with the conditional random field (FCN-CRF) network potential function with four convolutional layers tracked by CRF for structured learning.[29] Deep learning techniques based on CRF and Structured Support Vector Machine (SSVM) are used to propose the CAD system.[30] The mass segmentation is performed by using the statistical model, SSVM, is used for learning, Deep Belief Network (DBN) based on prior as potential function, Gaussian mixture model (GMM).[31]

Another deep learning CAD system based on deep structured output learning an active contour refinement level set method has been proposed to segment the mammogram images.[32] The RetinaNet algorithm is used to detect masses. To train and test the public INbreast and private GURO datasets the pre-trained weights are also used. The training set size is increased by using the data augmentation. The mammogram images are resized to 600 pixels. On the datasets, pre-trained weights are applied, which can influence the features learned by the dataset.[33] The segmentation and classification are performed using cascaded deep learning and Random Forests classifiers.[34]

The proposed CAD system for mammogram images used to detect, segments and classifies the images into a single framework. The Yolo is used to detect masses, and the full residual Convolution Network (FrCN) segments the masses. The masses are segmented using the CRF model and the Tree Re-weighted (TRW) belief propagation method, which helps to directly reduce segmentation errors by allowing the learning mechanism and inference mechanism to produce optimal results under TRW estimation.[8] The deep learning model full convolutional network (FCN) proposed to perform the segmentation.[35] To perform the masses segmentation U-NET model with attention gates is proposed.[36] To perform the mass mammogram segmentation the SAP_cGAN (Conditional Generative Adversarial Network) is used. To improve the segmentation boundary the superpixel average pooling layer is used in cGAN. The Dice coefficient for INbreast dataset is 91.54% achieved.[2] The mass segmentation is performed using the deep, fully convolution net with the potential function of the CRF (FCN-CRF) network with four convolutional layers tracked by CRF for structured learning.[29] The segmentation and classification are performed by using intuitionistic possibilistic Fuzzy c-mean clustering and fuzzy SVM algorithm.[37] The Vanilla-UNET model is proposed for mammogram segmentation. Images are segmented both with and without data augmentation. The DI, MIOU, and accuracy have been increased.[15]

As compared to traditional CAD systems based on conventional machine methods like seeded region growing, thresholding the deep learning models has become famous from the last few years. The segmentation and classification are performed by using the deep learning models. The CNN models are famously used for the segmentation of mammogram images. These CNN models are also used in the other medical fields to predict abnormal regions.[15,38] In the segmentation field, very few deep learning approaches have been applied. There is a need to explore segmentation by proposing new deep learning models and methods. In this way, the detection and segmentation of abnormal region will be more accurate.[39–41] To perform the segmentation the INbreast mass mammograms are used. The mixed-supervision guided method and a residual-aided classification U-Net model (ResCU-Net) is used. The dice coefficient 91.78% is achieved in the INbreast dataset.[42] The segmentation of the CBIS-DDSM and INbreast mass mammograms is performed by using the connected-UNets, connected-AUNETs and connected-ResUNets. The highest dice-score 95.28%, IOU is 91.03% in INbreast and dice-score 89.52%, IOU 80.02% in CBIS-DDSM is achieved by using the connected-ResUNets.[43] To perform the segmentation on INbreast and CBIS-DDSM dataset the deeply supervised U-Net model (DSU-Net) coupled with dense conditional random fields (CRFs) is proposed. The dice score for INbreast is achieved 79% and 82.9% is achieved for CBIS-DDSM.[44] The segmentation of mass mammogram is performed by using the residual UNET. The training is performed by using the CBIS-DDSM and BCDR-01. The testing is performed by using the INbreast dataset. The 94.4% accuracy and 90.5% dice index are achieved without augmentation of the dataset.[45] The segmentation of mass mammograms is performed by using the attention UNET. The dice coefficient is 81.8% is achieved in CBIS-DDSM and 79.1% is achieved in INbreast.[7]

In the segmentation field, most models just only the localization of the region from the mammogram images. These models only detect the region, not segment the masses or lesions from the mammogram images. The bounding box technique only detects the region, not segment the lesions. To identify the regions the region-based CNN models like R-CNN, Fast-RCNN, and Faster R-CNN models are also used. The detection of objects is performed. The CNN features are used for segmentation purposes. Low-level image features as well as high-level object detector features are employed.[46] The R-CNN models require more computation power and resources for training the images and detecting the features.[47] The Faster R-CNN approach is better than the R-CNN model.[48] The You Only Look Once (YOLO) approach is used to detect the mass region. Mass segmentation is not used in this study.[49]

AI:Pls check sentence structure
Please change this sentence as.
Most models simply recognize patches from mammography images.

Many studies are performing segmentation on data augmentation. The data augmentation approach is carried out to increase the size of dataset and to deal the class misbalancing scenario. The deep learning models generate good results when trained on larger datasets. The accuracy, dice index also increase when augmentation of the dataset is performed.[50] The segmentation of mass mammogram images is performed by using the Unet128 Adam. The IOU 90.50% is achieved for CBIS_DDSM and INbreast.[51] The segmentation of breast mass mammogram images is performed. The dice index 74.8% achieved in CBIS-DDSM by using pretrained U-Net+ResNet34.[52] The segmentation of masses is performed by using the cGAN. The 87.03% IOU and 94.07% dice index is achieved.[53] The study proposed that high-resolution images and large-size datasets produce better results than low-resolution images.[14] The mass detection is performed by using the Faster-RCNN on INbreast dataset.[54] The classification is performed on entire mass mammogram images by using the modified entropy whale optimization algorithm.[55]

In Table 1, some studies related to INbreast dataset segmentation approaches are explained with the dice index (DI), intersection over union (IOU) and accuracy.

In Table 2, the CBIS-DDSM dataset related approaches and results are explained. The dice index (DI), intersection over union (IOU), sensitivity and accuracy (Acc) are explained.

In Tables 1 and 2 studies related to INbreast and CBIS-DDSM dataset are presented. Some researchers also used private datasets to perform the segmentation.

Table 1. Studies related to INbreast dataset.

References	Year	Dataset	Number of Images	Methodology	Purpose	Results (%)
43	2021	INbreast	107	Connected-UNets, two UNets using additional modified skip connections, data augmentation	Segmentation	IOU: 91.03
7	2020	INbreast	107	AUNET	Segmentation	DI = 79.10
53	2020	INbreast	106	cGAN	Segmentation	DI: 68.69 IOU: 52.31
56	2020	INbreast	107	Attention mechanism and multiscale pooling adversarial network (AM-MSP-cGAN)	Segmentation	DI: 83.92 ± 5.81
44	2020	INbreast	107	DS U-Net coupled with dense CRF's	Segmentation	DI: 79.00
42	2019	INbreast	107	ResCU-Net, by incorporating residual module and SegNet	Segmentation	DI: 91.78
8	2018	INbreast	112	YOLO, full resolution convolutional network (FrCN), data augmentation	Detection, segmentation	Acc: 93.09 DI: 92.89
29	2018	INbreast	116	Full convolutional neural network by using conditional random field (FCN-CRF)	Segmentation	DI: 90.97
32	2017	INbreast	—	Deep structured output learning CRF by active contour refinement level set method	Segmentation	DI: 0.85
57	2015	INbreast	116	Tree re-weighted belief propagation	Segmentation	DI: 0.89
31	2015	INbreast	116	SSVM with potential functions	Segmentation	DI: 0.88

Table 2. Studies related to CBIS-DDSM.

References	Year	Dataset	Number of Images	Methodology	Purpose	Results (%)
43	2021	CBIS-DDSM	1467	Connected-UNets, two UNets using additional modified skip connections, data augmentation	Segmentation	IOU: 80.02
44	2020	CBIS-DDSM	857	DS U-Net coupled with dense CRF’s	Segmentation	DI: 82.90
56	2020	CBIS-DDSM	795	Attention mechanism and multiscale pooling adversarial network (AM-MSP-cGAN)	Segmentation	DI: 84.49 ± 0.43
58	2020	CBIS-DDSM	152	Coarse segmentation and fine segmentation by using HRAK	segmentation	Sensitivity: 90.85
7	2020	CBIS-DDSM	858	AUNET	Segmentation	DI = 81.80
36	2019	DDSM	400	Dense-UNet, data augmentation	Segmentation	Acc: 78.38 DI:= 82.24 ± 0.06
59	2019	CBIS-DDSM	1592	DCNN, inception V3 CNN, VGG 16, ResNet50, transfer learning, data augmentation	Detection	Acc: 84.16 ± 0.19

3. Methodology

The proposed methodology is detecting and identifying breast abnormal regions from mammographic images. The INbreast and CBIS-DDSM dataset are firstly preprocessed to enhance the clarity of the images. The two semantic networks are used to perform the segmentation. The one model approach is semantic network that is only used to check its effects on the dataset and other proposed approach is skipping dilation semantic network. These networks are applied on the datasets that have different architect of layers with the same kernels. However, the dilation factor and skipping connections are introduced further in the proposed network. This dilation factor increased squarely on incoming convolves layers. It ultimately increased the mean global accuracy, mean intersection over union (IoU), and BF-Score. The segmented results are extracted from both datasets by applying these two models. The results of proposed skipping dilation are more promising. The accuracy, weighted IOU (WIOU), mean-IOU (MIOU) results of proposed network are more promising. The proposed skipping dilation semantic CNN methodology of the segmentation is given below.

Figure 1 depicts the segmentation of the two case studies, CBIS-DDSM and INbreast datasets. Preprocessing of the images is carried out. Following preprocessing, the segmentation results of the two models CNN without skipping dilation and CNN with skipping dilation are presented. The segmented results with the skipping dilation factor-based CNN network are more promising than the segmented results without a dilation factor-based semantic CNN network, as shown in the below figure.

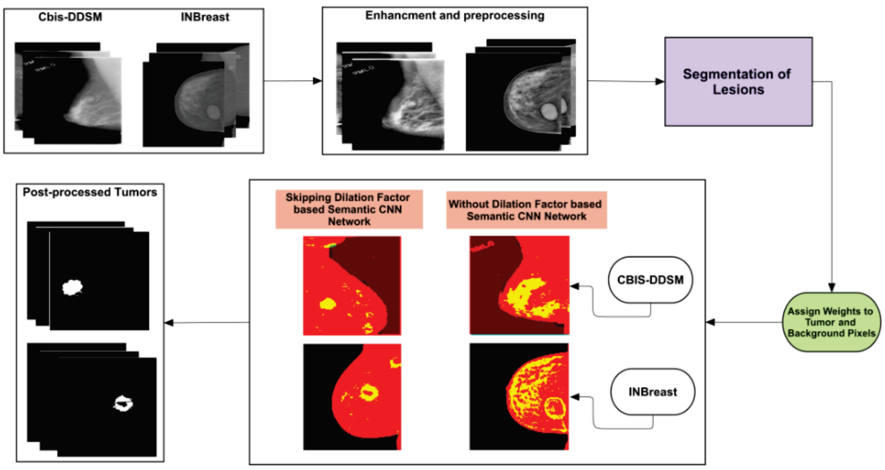

Fig. 1. Proposed framework for mammography masses segmentation.

3.1. *Data description*

In the proposed framework, two datasets have been used. INbreast and CBIS-DDSM are two well-known mammography datasets. It contains the ground truth values for lesions region annotations. The details of both datasets are provided on page 2340012-11.

(i) **CBIS-DDSM**

The CBIS-DDSM is a more recent version of the DDSM. The DDSM is a database containing 2620 mammography films. The data consists of benign, malignant with validated ground truth values for the development of CAD systems; however, the DDSM dataset is stored in non-standard compression files that are unreadable and inaccessible without the decompression code, which is no longer available or obsolete.

ROI annotations indicating the general position of the lesions but not accurate segmentation are possible by using DDSM dataset. The CBIS-DDSM dataset is organized by trained mammographers and is a standardized form of the DDSM dataset that is now used by the researchers. The images are in dicom format. Annotations, updated ROI, and data for training pathological information are all available.[13,44] In this study the 1592 masses images used. The CBIS-DDSM mass images include complete pathology, BIRADS, abnormality, and ground truth information. The 1231 images used for training and 361 images are used for testing.

(ii) **INbreast**

There are 410 images in the INbreast dataset. The full field digital mammogram (FFDM) 343 ROI images are included in the INbreast dataset. There are 115 patients who have craniocaudal (CC) and mediolateral oblique (MLO) views of their left and right breasts, respectively. The breast is a digital mammogram that covers the entire field of view.[12] Depending on the image acquisition process, the two sizes are $3328*4084$ of 167 images and $2560*3328$ of 243 images, according to the patients' breast size.

The BI-RADS for the dataset is provided. The INbreast dataset includes 107 mass images with ground truths.[31] Mass images 107 are used to segment masses.

INbreast and CBIS-DDSM, both dataset's training and testing for segmentation, is performed by classifying the pixels into background and tumor classes. The 80% data is utilized for training and 20% data is utilized for testing according to given benchmark.

3.2. *Preprocessing of the dataset*

The data has been enhanced, and noise has been removed. Figure 2 describe the results of before and after of preprocessed data. The original images are enhanced using unsharp masking and the contrast adaptive histogram equalization (CLAHE) method to enhance and remove noise from the images properly. In Fig. 2, the histogram for both the original and enhanced images shows that the image intensities are distributed evenly.

CLAHE improves image contrast by computing each block transformation function where images are divided into non-overlapping $n*n$ blocks. The size of the clip limit is kept small to remove the noise[44] It will ultimately rise to get more helpful information. The input image is inp_{img}, the number of tiles nt by default set [8 8], the contrast enhancement limit (cel) is mentioned that is between the range of [0 1]. The shape of the histogram ($hists$) is mentioned. The range (ran) of the output image is mentioned. The entire image range is between (0, 255) and the original is between the image's

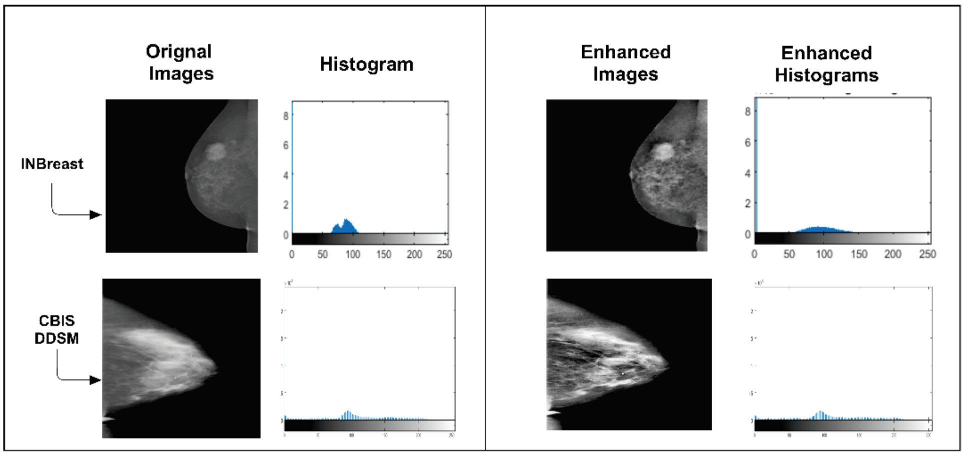

Fig. 2. Original and enhanced images with histogram.

minimum to a maximum value. The equation of CLAHE is given below.[60]

$$cle = [inp_{img}, nt, cel, hists, ran] \tag{1}$$

The unsharp masking method is used to create the mask of the blurry original images. The radius, amount, and threshold values govern the unsharp masking method. The radius can be as small or as large as the image's sharpness requires. Different filters are used to unsharp the images, like median, mean, Laplacian, Gaussian, etc. The unsharp masking equation is given below.[61]

$$usm = (inp_{img} + (inp_{img} - blur) * amt \tag{2}$$

To adjust the image edge borders lighter and darker, there is a need to set the magnitude and percentage of the edges. This is performed by using the *amt* parameter. The number of edges is represented to show the darkness and lightness of the edges. The *amt* is used to describe the percentage and control the magnitude of each edge contrast. This deals with the contrast of the edges.

3.3. *Introduction semantic CNN and skip dilated semantic CNN*

The traditional CNN comprises several layers, including an input layer, convolutional layers, and an output layer. The difference is that CNN's input an image in a pixel matrix, whereas the output calculation is the image features obtained through convolution.[62] The convolution kernel is the essential component in the CNN model, and the CNN is the source of this term. The two-dimensional matrix with $n * n$ points and weights represent the convolution kernel. A convolution kernel is related to a neuron, and the neuron's receptive fields determine the size of the convolution kernel.

The CNN model uses the K convolution kernels calculation to input the image and perform the calculation. It means that the image position's weight values and pixel values are added within the receptive field. To pick the next position of the image the convolution kernels are then moved to the next step size and to count all of the pixels in the image, the process is repeated until all computation is completed. The original image's feature maps are the output pixel matrix, and feature maps *K* is produced by the convolution kernels *K*. The pooling layers in the semantic CNN are important layers because it preserves the information by minimizing the image size. To adjust the fitting ability of the CNN, the nonlinear factors are included. Different nonlinear activation functions are used like ReLU, sigmoid, but the ReLU can better simulate the CNN. There are lots of issues in the semantic CNN.

The pooling layer can miss minor pixel points of the image, and this may cause minimize the accuracy of the system. The CNN model depth increases by loading the layers, and this causes the gradients to disappear from the network due to the back-propagation gradient. These factors drenched the performance of the system. In the CNN, when more layers were added as the requirement of the network, the size of the parameters also increased, that increase the computation resources. To reduce these issues, the semantic dilated convolution model is proposed.[63]

3.4. *Proposed semantic skipping dilated CNN network for segmentation*

The convolution kernel gains the large size of the receptive due to the pooling operation, and this is not the compulsory part of the CNN,[64] and this is a result of major data loss[63] To allow each convolution output to hold sufficient information without pooling layer by using the dilated convolution that can expand the receptive field and solve problems requiring elongated sequence information. In this study, proposed the semantic skipping dilated CNN model for image segmentation to preserve image information. Using the 37 layers, the dilated CNN was applied to the images. The equation of dilated CNN model is given below.[63,65]

$$(f * df^k)(p) = \sum_{s+df^t=p} f(s)k(t) \tag{3}$$

The f is a discrete function that is expanded without losing any information. The df is the dilation factor, k is no of filters. The p is the receptive field element. Figure 3 represents the proposed skipping dilation semantic CNN network.

In Fig. 3, the architecture of semantic segmentation with skip dilation factor is presented. The ten significant blocks contain a sequence of convolves, batch normalization, and ReLU by assigning the dilation factor are presented. The kernel size and number of filters are shown in Table 3. Each convolve layer and its respective learned weights are mentioned in Table 3. In this paper two semantic segmentation models used. In the proposed semantic segmentation model, dilation factor and skipping connections are used by increasing the number in each coming convolve layer for comparison. The semantic segmentation CNN model without skipping dilation factor is used just to check the efficiency. The visual results and dilation factor role is presented in Fig. 4. The *W* parameter signifies the weights, *BI* denotes the bias, *OS* signifies the offsets, and *SC* signifies the scale.

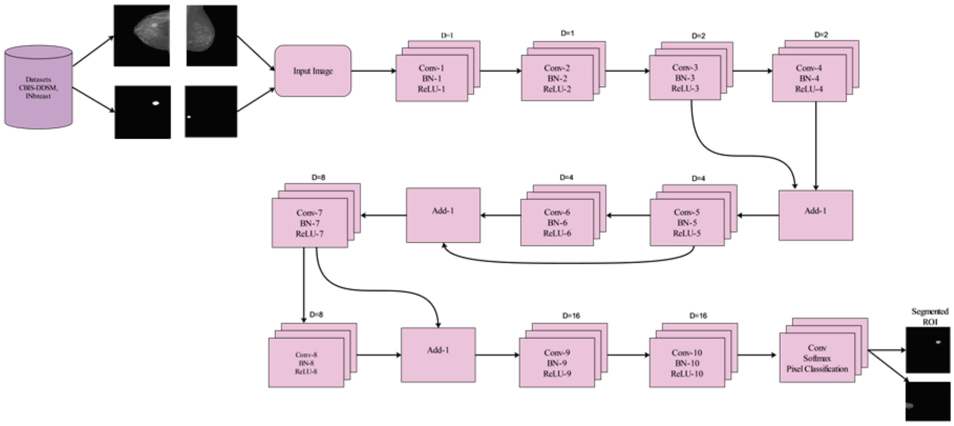

Fig. 3. Semantic CNN architecture with skipping dilation factor.

In Table 3, the proposed skipping dilation semantic CNN architecture is presented. The detail of layers, activations, kernel size, stride, dilation factor, learned parameters and feature maps are presented in Table 3. We applied different combinations of layers and then finalized the proposed model. The total 37 layers are used in the proposed skipping dilation semantic CNN. The one layer is image input layer. The eleven layers are convolution layers. The ten ReLU, ten batch normalization layers, three skipping add layers, one Softmax and one output layer is used.

This study proposed the skipping dilation semantic CNN architecture for the breast cancer mammography segmentation. The 37 layers used according to our proposed framework. The types of layers and selected layers numbers are all determined by the data and application. The details of each layer and its parameters details theoretically have been explained in the coming sections.

3.4.1. *Image input layer*

This layer mentions the image size using the input size argument. The size of the image is according to the height, width, and number of the colors. The channels are mentioned in the image. Channel 1 is used for the gray level image. The resizing of the images is done in the preprocessing phase. The size of images kept 512∗512. The image input layer's purpose is to send images to a network and then normalize the data.

3.4.2. *Convolutional layer*

To apply the convolutional filters to the images, the 2-D convolutional layers are used. For the small network, the two convolution layers are sufficient. Multiple convolutional and fully connected layers are required for complex networks and datasets. The proposed framework employs eleven convolutional layers. Convolutional layers neurons are used to connect the sub-regions of the input images or the previous layer's outputs. These

Table 3. Proposed skipping dilation semantic CNN architecture.

No.	Layers	Activations	Kernel Size	Stride	Dilation Factor	Learned Parameters	Feature Maps
1	Image input	512∗512∗1	—	512∗512	—	—	—
2	Conv_1	512∗512∗32	5∗5	[1 1]	[1 1]	W: 5∗5∗1∗32 BI: 1∗1∗32	32
3	BN_1	512∗512∗32	—	—	—	OS: 1∗1∗32 SC: 1∗1∗32	32
4	R_1	512∗512∗32	—	—	—	—	—
5	Conv_2	512∗512∗32	5∗5	[1 1]	[1 1]	W: 5∗5∗32∗32 BI: 1∗1∗32	32
6	BN_2	512∗512∗32	—	—	—	OS: 1∗1∗32 SC: 1∗1∗32	32
7	R_2	512∗512∗32	—	—	—	—	—
8	Conv_3	512∗512∗32	5∗5	[1 1]	[2 2]	W: 5∗5∗32∗32 BI: 1∗1∗32	32
9	BN_3	512∗512∗32	—	—	—	OS: 1∗1∗32 SC: 1∗1∗32	32
10	R_3	512∗512∗32	—	—	—	—	—
11	Conv_4	512∗512∗32	5∗5	[1 1]	[2 2]	W: 5∗5∗32∗32 BI: 1∗1∗32	32
12	BN_4	512∗512∗32	—	—	—	OS: 1∗1∗32 SC: 1∗1∗32	32
13	R_4	512∗512∗32	—	—	—	—	—
14	Add_1	512∗512∗32	—	—	—	—	—
15	Conv_5	512∗512∗32	5∗5	[1 1]	[4 4]	W: 5∗5∗32∗32 BI: 1∗1∗32	32
16	BN_5	512∗512∗32	—	—	—	OS: 1∗1∗32 SC: 1∗1∗32	32
17	R_5	512∗512∗32	—	—	—	—	—
18	Conv_6	512∗512∗32	5∗5	[1 1]	[4 4]	W: 5∗5∗32∗32 BI: 1∗1∗32	32
19	BN_6	512∗512∗32	—	—	—	OS: 1∗1∗32 SC: 1∗1∗32	32
20	R_6	512∗512∗32	—	—	—	—	—
21	Add_2	512∗512∗32	—	—	—	—	—
22	Conv_7	512∗512∗32	5∗5	[1 1]	[8 8]	W: 5∗5∗32∗32 BI: 1∗1∗32	32
23	BN_7	512∗512∗32	—	—	—	OS: 1∗1∗32 SC: 1∗1∗32	32

(*Continued*)

Table 3. (*Continued*)

No.	Layers	Activations	Kernel Size	Stride	Dilation Factor	Learned Parameters	Feature Maps
24	R_7	512∗512∗32	—	—	—	—	—
25	Conv_8	512∗512∗32	5∗5	[1 1]	[8 8]	W: 5∗5∗32∗32 BI: 1∗1∗32	32
26	BN_8	512∗512∗32	—	—	—	OS: 1∗1∗32 SC: 1∗1∗32	32
27	R_8	512∗512∗32	—	—	—	—	—
28	Add_3	512∗512∗32	—	—	—	—	—
29	Conv_9	512∗512∗32	5∗5	[1 1]	[16 16]	W: 5∗5∗32∗32 BI: 1∗1∗32	32
30	BN_9	512∗512∗32	—	—	—	OS: 1∗1∗32 SC: 1∗1∗32	32
31	R_9	512∗512∗32	—	—	—	—	—
32	Conv_10	512∗512∗32	5∗5	[1 1]	[16 16]	W: 5∗5∗32∗32 BI: 1∗1∗32	32
33	BN_10	512∗512∗32	—	—	—	OS: 1∗1∗32 SC: 1∗1∗32	32
34	R_10	512∗512∗32	—	—	—	—	—
35	Last_Conv	512∗512∗32	1∗1	[1 1]	—	W: 1∗1∗32∗2 BI: 1∗1∗2	2
36	Softmax	512∗512∗32	—	—	—	—	—
37	Class output	Pixel classification	—	—	—	—	—

regions are used by the layers to learn features as they scan through an image. The dot product is computed by combining the weights, input, and bias of each region. Filters are applied to the region as the set of weights. The number of parameters minimized by convolutional neural network by using fewer connections, shared weights, and down-sampling.[66] Depending on the needs of the network, different components are used in the convolutional layer. In this study, we used the following components in our proposed semantic skipping dilation CNN network.[62,67]

3.4.2.1. Filters

The filters are applied to the images region in the form of set of weights. To compute the regions of images the filters move vertically and horizontally. The 5∗5 filters are used in the convolutional layer. Stride refers to the size of the step along with the filter move. The [1 1] stride is used in the proposed network.

3.4.2.2. Weights

In a filter, the number of weights is the height h, width wd, and number of channels c in the input image. The weights equation is given below.

$$W = h * wd * c \tag{4}$$

3.4.2.3. Dilation factor

The dilation factor method expands the space between the filter's elements. The zero is inserted between each factor. To find the step size for input sampling or up-sampling the filter factor equivalently, the dilation factor is applied. The dilation factor equation is given below.

$$dfc = (fz - 1) * df + 1 \tag{5}$$

In the dilation factor equation, the fz parameter is filter size, and df is the dilation factor.

3.4.2.4. Feature maps

To generate the feature maps the filter moves along the input, using the same weight and bias as the convolution. The feature map is the result of various weightings and biases. The features from the input image are captured by feature map' s. The equation is given below.

$$FM = (W + BI) * k \tag{6}$$

In this equation, the W is weight, BI is a bias that is used one and k are number of filters used to calculate the feature maps.

3.4.2.5. Learned parameters

The learned parameters can be used by defining the parameters locally. If not defined locally, then the network uses global training options.

3.4.2.6. Inverse frequency weighting

Inverse frequency weighting[64, 68] is a weighting technique that is commonly used. Each class is weighted based on the frequency of the class. The number of pixels inversely proportional to the weight. The target objects become heavier as their size decreases. The inverse frequency weight is calculated as follows:

$$wc^{inverse} = \frac{1}{\left(\sum_{i=1}^{N} \beta, c\right)} \alpha \tag{7}$$

The power parameter is represented by α used for the cross-entropy loss function and loss function is represented by β. The weighted inverse of square frequency is generalized dice loss.

3.4.3. *Batch normalization layer* (*BN*)

The processing of a small batch of data across all observations for each channel separately is called batch normalization. The batch normalization and ReLU layers are used to improve training while decreasing the sensitivity of network initialization. The training speed can be increased by increasing the learning rate. The parameters update rate and network learn rate can both be increased. Batch normalization has characteristics such as trained mean, trained variance, and several input channels. Offset, Scale, Mean Decay, and Variance Decay are some of the parameters used in the batch normalization layer.[69]

3.4.4. *Rectified linear unit* (*ReLU*)

The ReLU layer is responsible for performing threshold operations on each input element. The value is set to zero that is less than zero. Convolutional and batch normalization layers are the ReLU layer. The size of input image is not affected by ReLU. The ReLU equation is given below.[70]

$$f(x) = \begin{cases} 0, & x < 0 \\ x, & x \geq 0 \end{cases} \tag{8}$$

3.4.5. *Softmax function*

The Softmax activation function is defined by

$$y_r = \frac{\exp(\alpha_r(x))}{\sum_{j=1}^{k} \exp(\alpha_j(x))} \tag{9}$$

The Softmax function is a multiclass generalization of the logistic sigmoid function and also known as normalized exponential.[70] In the classification network the classification layer must come after the Softmax layer. In the classification layer, the network uses the cross-entropy function to K equally elite classes, based on values from the Softmax function for a 1 of K coding scheme.[70]

$$l = \frac{-1}{sam} \sum_{i=1}^{sam} \sum_{i=1}^{cl} w_i t_{ni} \ln y_{ni} \tag{10}$$

The number of samples are represented by sam, number of classes shows by cl, w_i is used to symbolize the weight for class l, t_{ni} is used to represent that nth samples relates to the class, and y_{ni} is the output for sample n for class l which is the value from the Softmax function. The network links the nth input with class l in the probability of y_{ni}.

3.4.6. *Output layer*

The output layer is the final layer, which displays the segmented tumor. The predicted tumor is the segmented tumor, which is evaluated using deep learning models.

3.4.7. *Skipping layer*

The skip layer is use to fed the one layer output to the other layer as an input. It increases the efficiency and performance of the system.

3.5. *Design semantic segmentation CNN without skipping dilated CNN*

CNN sequentially performs convolution and pooling operations. The pooling operation input is based on output of convolution operations that is fed into it, and next convolution layer input is based on the pooled layer's results and so on until it reaches the Softmax layer. To deal with input data in the convolutional layer CNN uses the convolution kernel. To extract the local features each convolutional layer is connected to the previous layer's data in the local receptive field. The differential features are extracted by each convolution kernel in turn. Convolution is used because the data obtained after a convolution kernel's operation is a feature map. The performance of deep neural network for nonlinear transformation in deep learning is improved by using the Rectified Linear Unit (ReLU) function. The scale-invariant feature transform is obtained by aggregating the local features of a specific region in the pooling layer. The computational cost and dimensions of processing data are minimized by pooling operations while extracting useful information.[11,71]

Batch Normalization (BN) has been proposed as a method of improving CNN performance[69] The BN layer has the potential to improve data distribution and speed up model training. Furthermore, by preventing over-fitting and gradient disappearance during training, the BN layer improves network generalization.[7] The semantic CNN equation without the dilated factor is given below[63,65]

$$(F * k)(p) = \sum_{s+t=p} F(s)k(t) \tag{11}$$

The semantic CNN architecture is used without using the skipping dilation factor. The dilation factor, weights are not assigned to the semantic CNN model. The simple deep learning model CNN is applied. The skipping dilation factor is not applied in the semantic CNN model. This model is just use to check the accuracy of the system.

In the proposed skipping dilated semantic CNN model the layers are increased step by step and then finalized the proposed model. The skipping dilation factors are assigned to the semantic CNN model to increase the performance and system's efficiency.

3.6. *Data post processing*

The post-processing of the segmented images is performed to identify the specified lesion of the entire context. The predicted results can be effective by the neighborhood dependencies, so there is a need to separate the background pixels from the foreground pixels in the probabilistic graphical models.[44,53]

The CNN results of skipping dilated and non-dilated CNN are different. The skipping dilated CNN has much clearer predictions regarding tumors in the given image. The noise is removed using an area-wise selection of tumors in the given image. The area-wise selection is controlled by using the given below equation.

$$s_8 = \max(|y_i - y_j|, |z_i - z_j|) \tag{12}$$

$$s_4 = |y_i - y_j| + |z_i - z_j| \tag{13}$$

The y and z are the pair pixels and i, j are the labels.

After post-processing of the given predicted mask of CNN, the predicted mask of tumors are much clearer as shown in Fig. 4.

The segmented results of INbreast dataset are shown in Fig. 4. The segmentation of the masses is performed by using semantic CNN with the skipping dilation factor and semantic CNN without the skipping dilation factor. The masses of various shapes and sizes are predicted after applying post-processing methods that include morphological operations to remove noise from images to separate the segmented mass. From the figure, it can be seen that masses prediction is best by using the skipping dilated semantic CNN with the weights as compared to the semantic CNN without the skipping and dilation.

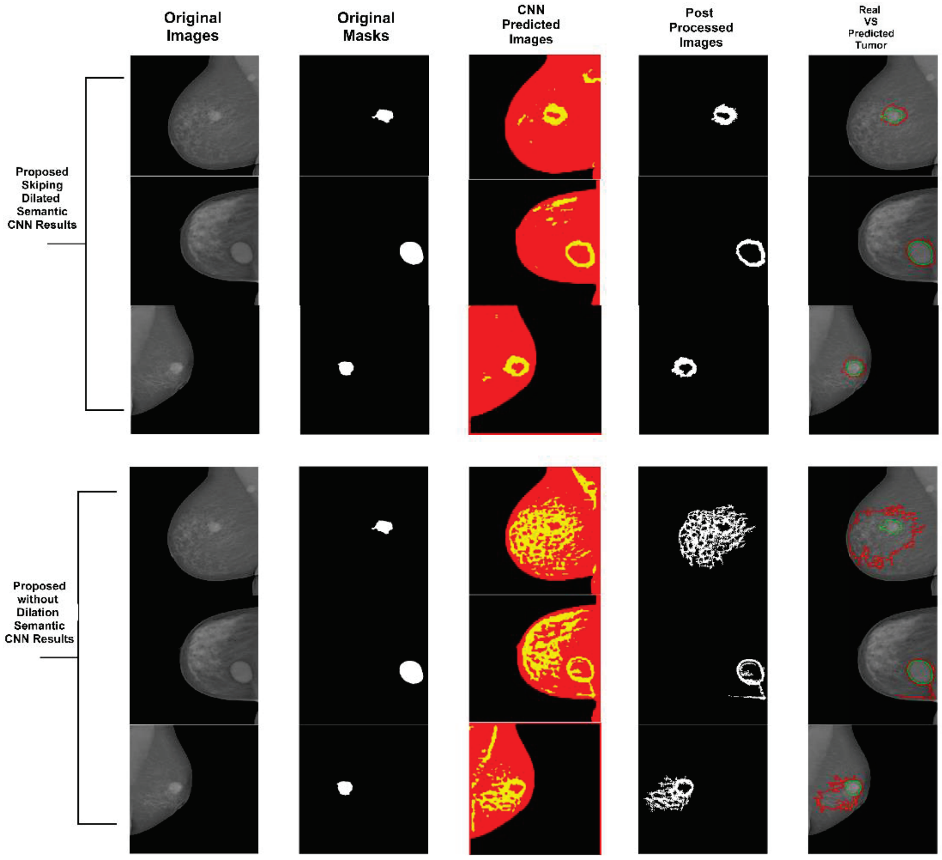

Fig. 4. Segmented results of INbreast dataset with and without skipping dilation factor.

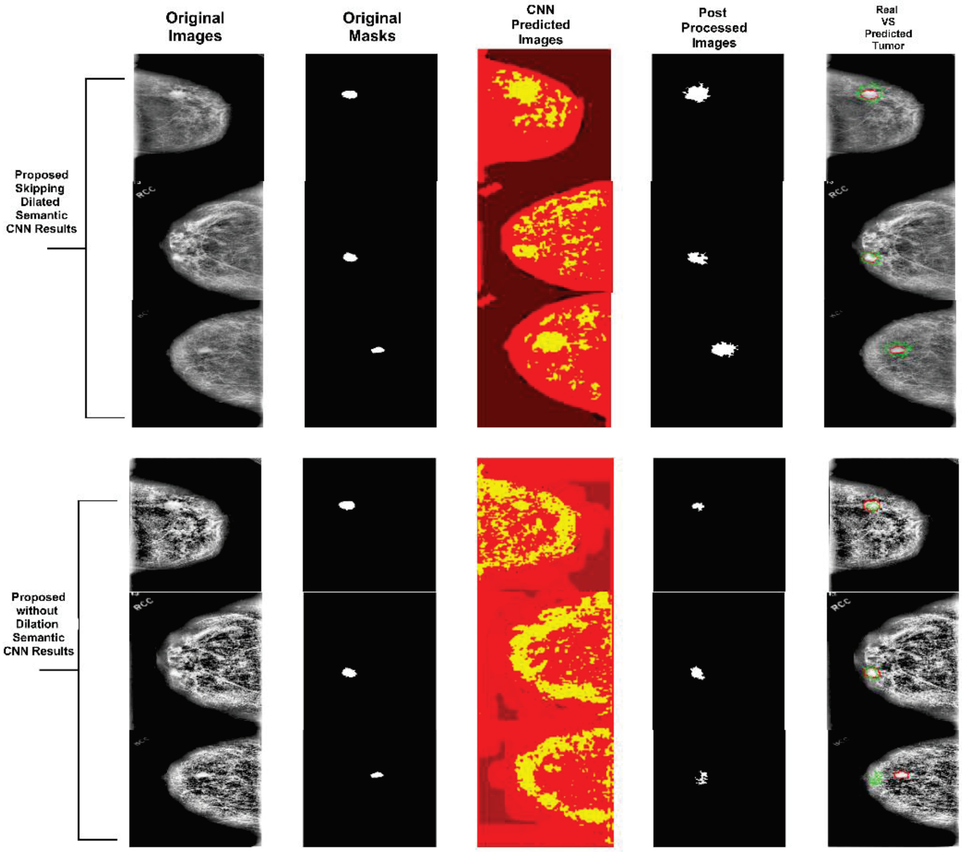

Fig. 5. CBIS-DDSM dataset results with skipping dilated semantic segmentation and without dilation factor.

The pectoral muscle is also removed from the segmented results of the masses. The predicted results also mapped with the ground truths (GT).

In Fig. 5, the CBIS-DDSM model is trained by using the masses dataset. The 80% data is used for training, while 20% is used for testing. Figure 5 presented the predicted outcomes of both models. To predict the masses from the images, post-processing morphological operations are used. The actual ground truth image and predicted results are mapped after post-processing. The red color image shows the GT result and the green color show the predicted results. The last mass prediction figure shows that ground truth and predicted mass are not mapped by applying the CNN model without dilation. The skipping dilation prediction results are best as compare to the CNN model.

Figures 4 and 5 depict the predicted results of semantic segmentation with and without dilation CNN using the INbreast and CBIS-DDSM datasets. The proposed skipping dilated CNN model can more precisely predict mass segmentation results. The above figure presented that pectoral muscles have been removed and precise segmentation of the masses has been performed.

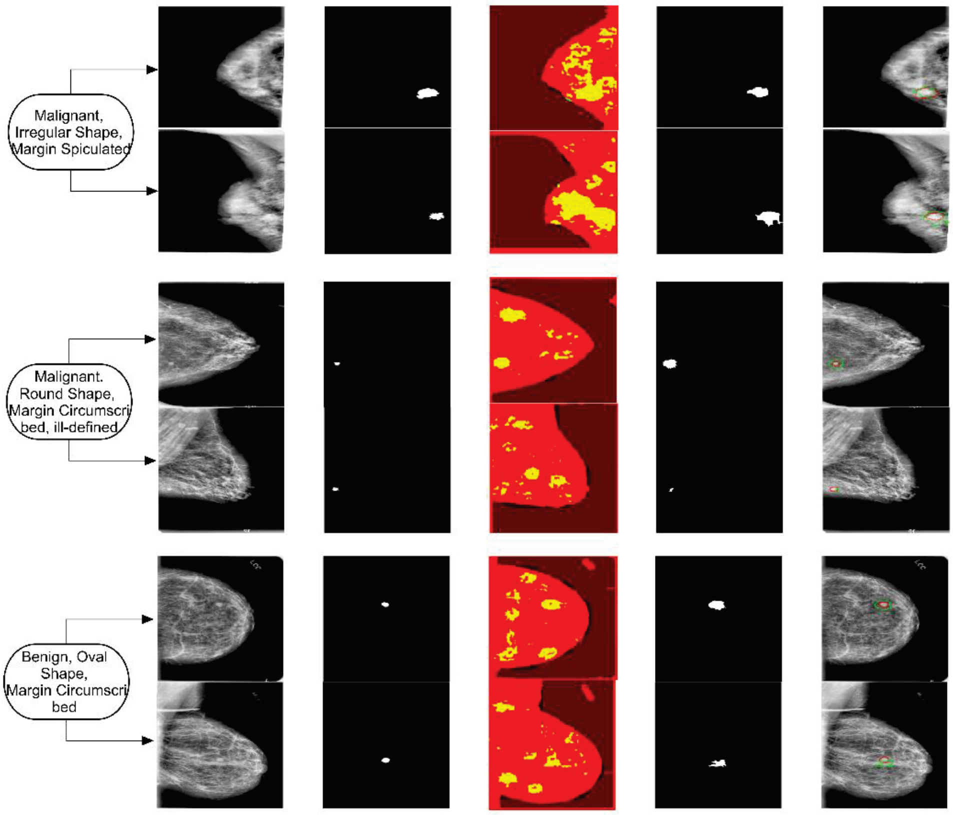

Fig 6. CBIS-DDSM masses shapes predicted by semantic skipping dilated CNN model.

Figure 6 depicts the different malignant and benign masses segmented shapes from the CBIS-DDSM dataset. The irregular, round malignant shapes with speculative, circumscribed, and ill-defined margin types are presented. The benign oval shape with circumscribed margins is shown. The masses of various shapes, locations, and margin types can be predicted by using the proposed model.

In Table 4, the proposed semantic skipping dilated CNN results of INbreast and CBIS-DDSM are shown. The global accuracy, Dice Index (DI), and BF-Score of the INbreast and CBIS-DDSM dataset is presented.

Table 4. Skipping semantic dilated CNN results of INbreast and CBIS-DDSM segmentation.

Dataset	Accuracy/Precision	WIOU	BF-Score
INbreast	98.95%	98.51%	77.59%
CBIS-DDSM	95.39%	94.82%	43.54%

4. Experimentation and Results

Using the CLAHE, the proposed study first preprocessed input data to improve the images. After preprocessing, use the proposed skipping dilated CNN architecture to perform segmentation. The skipping and dilated factor involved CNN and CNN without skipping dilation factor models are used for comparison. Both semantic CNN results are presented in Table 5. The segmentation results evaluation performed according to global mean accuracy, mean IOU (MIOU), weighted intersection over union (WIOU), and BF-Score. Both models were run for 100 epochs and a learning rate of 0.0001. The Matlab 2021a, is used for computation.

4.1. *Semantic CNN segmentation results and comparison*

In Table 5, the training and testing results with the skipping dilated CNN-based model and without skipping dilated CNN-based models presented. The global accuracy of the INbreast dataset is 98.95% and the weighted IOU (WIOU) is 98.51%. When compared to the traditional CNN model, this weighted IOU and accuracy are the best. In Table 5, the global accuracy (GA), mean accuracy (MA), Mean intersection over union (MIOU), Weighted Intersection over Union (WIOU), and mean F1 score is calculated that is described by (M-BFScore).

The CBIS-DDSM dataset's results are shown in Table 6. The table shows that our proposed model outperforms the CNN model without the dilated factor in terms of global accuracy and weighted IOU. The WIOU is 94.82% and global accuracy is 95.39%. The testing and training results of dilated semantic CNN and without dilated semantic CNN are presented.

Different studies of the INbreast dataset are presented in Table 7. The comparison shows that the result of proposed method is better from the other studies.

In Table 8, different CBIS-DDSM studies are presented along with their dice index. Most studies used a smaller number of images. it is observed that some studies performed data augmentation for masses segmentation.[10,2] In this study, data augmentation did not perform for mass segmentation.

Table 5. Semantic segmentation CNN predicted results on INbreast dataset.

Method	GA	MA	MIoU	WIoU	M-BFScore
Proposed skipping dilated factor-based CNN (Training data)	0.98628	0.95675	0.71543	0.97971	0.82455
Proposed skipping dilated factor based CNN (Testing data)	0.98957	0.88577	0.66226	0.98512	0.77591
Non-skipping dilated factor-based semantic CNN (Training data)	0.90054	0.67806	0.45067	0.90037	0.14007
Non-skipping dilated factor-based semantic CNN (Testing data)	0.9071	0.67068	0.45382	0.90699	0.14715

Table 6. Semantic segmentation CNN predicted results on CBIS-DDSM dataset.

Method	GA	MA	MIoU	WIoU	M-BFScore
Proposed skipping dilated factor-based CNN (Training data)	0.95705	0.90943	0.53715	0.95123	0.44747
Proposed skipping dilated factor-based CNN (Testing data)	0.95392	0.88377	0.52736	0.94824	0.43543
Non-skipping dilated factor-based semantic CNN (Training data)	0.9154	0.66666	0.45794	0.91531	0.12027
Non-skipping dilated factor-based semantic CNN (Testing data)	0.91008	0.66071	0.45525	0.90999	0.11721

Table 7. Comparisons of INbreast segmentation with other studies.

References	Year	Dataset	Methodology	DI/IOU/WIOU
57	2015	INbreast	CRF and tree re-weighted (TRW) belief propagation	89%
30	2015	INbreast	CRF, SSVM	90%
32	2017	INbreast	CRF model with active contour refinement	85% ± 0.02
8	2018	INbreast	FrCn	92.69%
29	2018	INbreast	FCN-CRF	90.97%
7	2020	INbreast	AUNET	79.1% ± 6.0
72	2020	INbreast	Multiscale adversarial networks	81.64%
44	2021	INbreast	(DS-UNET) model with (CRF)	79%,
2	2021	INbreast	cGAN with a pooling layer	91.54%
73	2021	INbreast	Adaptive channel and multiscale spatial context (ACMSC)	84.11%
Proposed	2021	INbreast	Skipping dilated semantic CNN	98.5%

Table 8. Comparisons of CBIS-DDSM segmentation results with other studies.

References	Year	Dataset	Methodology	DI/IOU/WIOU
7	2020	CBIS-DDSM	AUNET	81.8%
72	2020	CBIS-DDSM	Multiscale adversarial networks	82.16%
9	2020	CBIS-DDSM	Deep lab, mask-R-CNN	80.0%, 0.75%
44	2021	CBIS-DDSM	(DS-UNET) model with dense CRF	82.7%
10	2021	CBIS-DDSM	Mask-RCNN, data augmentation	75.0%
73	2021	CBIS-DDSM	ACMSC	82.81%
Proposed method	2021	CBIS-DDSM	Skipping dilated semantic CNN	94.82%

5. Discussion

Many studies have been conducted to develop CAD systems for breast masses segmentation, but most CAD systems are based on thresholding and seeded region growing methods. Most CAD systems used manual annotations for the datasets that gives the better results.[9] Many studies make use of non-comparable private datasets. There are few datasets with annotations for mammogram images that are publicly available. The comparison of the proposed method is performed, with other models that also used these two publicly available datasets. The preprocessing was done in order to enhance the visualization of the images in the dataset. The CLAHE is used to enhance the images. The deep learning model performs the segmentation to predict the masses from the images by eliminating the pectoral muscle. The background artifacts are automatically removed from the region of interest.

The images in the dataset are converted into jpeg form. These are resized into 512∗512 pixels to ensure uniformity using the cubic interpolation method. This way the information of the neighboring pixels is not lost. Many studies convert the dataset into png or jpeg format before resizing it. Resizing is performed in order to adjust the size of the mammograms. The large size of the mammogram images necessitates extensive computation resources. Our proposed model can achieve improved results with increased number of images. On the dataset, data augmentation is not performed. Some researchers do the data augmentation because the deep learning model performs better on larger datasets; the augmentation can increase the size of the dataset. The proposed semantic skipping dilation CNN and semantic CNN without skipping dilation factor two methods are used to perform the segmentation without augmentation. The comparison with the results shows that proposed skipping dilated semantic segmentation CNN results are more promising as compared to the semantic CNN segmentation without skipping dilation factor. In the proposed skipping dilation semantic CNN more layers are added step by step. The three skip connections are added. The Convolution and Batch normalizations layers are added. The total 37 layers are added in the proposed skipping dilated semantic CNN model.

6. Conclusion and Future Work

The breast cancer is a fatal disease all over the world and mostly females are victimized of this disease. The mortality rate among the women is high all over the world due to this disease. The early diagnosis of this disease can cure the life due to better treatment at an early stage. To provide the treatment in an initial step, it is necessary to diagnose the mammography images. The segmentation of the breast mass mammogram images is a challenging task all over the world due to low contrast images, irregular shapes, sizes and locations of the masses. Mostly studies only detect the abnormal region not perform the segmentation. In this proposed work, the segmentation of breast mass mammogram images is performed. It is confirmed that the proposed model results are more outstanding as compared to the other model.

In this paper, proposed a skipping semantic CNN segmentation model with a dilation factor to segment two publicly available datasets, INbreast and CBIS-DDSM. The semantic segmentation without skipping and dilation factor is also used to perform the segmentation. The two models semantic CNN model with and without the dilation factor is used to segment the data. The comparison of both models shows that the proposed skipping dilated semantic CNN performs better than the other model. The segmentation results show that the weighted IOU of semantic CNN with skipping dilation factor has outperform as compare to the semantic CNN model without the skipping and dilation factor, because detection of various shapes, locations, and sizes of the masses, segmentation breast masses from mammogram images is difficult. The precise segmentation of the mass mammogram images is performed from the mammogram images. There is no similarity of segmented results with the other parts like pectoral muscle of the breast organs. The proposed model segmentation results are compared with the other segmentation studies. The comparison with the other studies shows that the proposed method skipping dilation semantic CNN in the form of (WIOU) and global accuracy is better. The proposed method can be used to segment abnormal masses in other medical imaging fields. In future work, the augmentation of the dataset will be performed and new segmentation methods will be proposed to segment the results with high accuracy and precision.

Conflict of Interest

There is no conflict about this paper.

References

1. H. Sung *et al*., Global cancer statistics 2020: GLOBOCAN estimates of incidence and mortality worldwide for 36 cancers in 185 countries, *CA: A Cancer Journal for Clinicians* **71**(3) (2021) 209–249.
2. Y. Li *et al*., SAP-cGAN: Adversarial learning for breast mass segmentation in digital mammogram based on superpixel average pooling, *Medical Physics* **48**(3) (2021) 1157–1167.
3. S. Zahoor *et al*., Breast cancer detection and classification using traditional computer vision techniques: A comprehensive review, *Current Medical Imaging* **16**(10) (2020) 1187–1200.
4. B. Mughal, M. Sharif and N. Muhammad, Bi-model processing for early detection of breast tumor in CAD system, *The European Physical Journal Plus* **132**(6) (2017) 1–14.
5. E. Kozegar *et al*., Assessment of a novel mass detection algorithm in mammograms, *Journal of Cancer Research and Therapeutics* **9**(4) (2013) 592.
6. J. S. Cardoso, I. Domingues and H. P. Oliveira, Closed shortest path in the original coordinates with an application to breast cancer, *International Journal of Pattern Recognition and Artificial Intelligence* **29**(1) (2015) 1555002.
7. H. Sun *et al*., AUNet: Attention-guided dense-upsampling networks for breast mass segmentation in whole mammograms, *Physics in Medicine & Biology* **65**(5) (2020) 055005.
8. M. A. Al-Antari *et al*., A fully integrated computer-aided diagnosis system for digital X-ray mammograms via deep learning detection, segmentation, and classification, *International Journal of Medical Informatics* **117** (2018) 44–54.
9. L. Ahmed *et al*., Images data practices for semantic segmentation of breast cancer using deep neural network, *Journal of Ambient Intelligence and Humanized Computing* (2020) 1–17.
10. S. K. Raza *et al*., Classification and segmentation of breast tumor using mask R-CNN on mammograms (2021).
11. X. Lei, H. Pan and X. Huang, A dilated CNN model for image classification, *IEEE Access* **7** (2019) 124087–124095.

12. I. C. Moreira *et al*., INbreast: Toward a full-field digital mammographic database, *Academic Radiology* **19**(2) (2012) 236–248.
13. R. S. Lee *et al*., A curated mammography data set for use in computer-aided detection and diagnosis research, *Scientific Data* **4**(1) (2017) 1–9.
14. K. J. Geras *et al*., High-resolution breast cancer screening with multi-view deep convolutional neural networks, arXiv preprint arXiv:1703.07047 (2017).
15. D. Abdelhafiz *et al*., Convolutional neural network for automated mass segmentation in mammography, *BMC Bioinformatics* **21**(1) (2020) 1–19.
16. N. Muhammad *et al*., Image denoising with norm weighted fusion estimators, *Pattern Analysis and Applications* **21**(4) (2018) 1013–1022.
17. Y. M. Y. Abdallah, A. Hayder and E. Wagiallah, Automatic enhancement of mammography images using contrast algorithm, *Methods* **7**(8) (2014).
18. B. Sridhar, K. Reddy and A. M. Prasad, Mammographic image analysis based on adaptive morphological fuzzy logic CAD system, *International Journal of Biomedical Engineering and Technology* **17**(4) (2015) 341–355.
19. F. Zeng and L. Liu, Contrast enhancement of mammographic images using guided image filtering, in *Chinese Conf. on Image and Graphics Technologies* (Springer, 2013).
20. M. Sundaram *et al*., Histogram based contrast enhancement for mammogram images, in *2011 Int. Conf. on Signal Processing, Communication, Computing and Networking Technologies* (IEEE, 2011).
21. S. Mohan and M. Ravishankar, Modified contrast limited adaptive histogram equalization based on local contrast enhancement for mammogram images, in *Int. Conf. on Advances in Information Technology and Mobile Communication* (Springer, 2012).
22. T. K. Agarwal, M. Tiwari and S. S. Lamba, Modified histogram based contrast enhancement using homomorphic filtering for medical images, in *2014 IEEE Int. Advance Computing Conference* (*IACC*) (IEEE, 2014).
23. Q. Song *et al*., Image denoising based on mean filter and wavelet transform, in *2015 4th Int. Conf. on Advanced Information Technology and Sensor Application* (*AITS*) (IEEE, 2015).
24. H.-D Cheng *et al*., Automated breast cancer detection and classification using ultrasound images: A survey, *Pattern Recognition* **43**(1) (2010) 299–317.
25. A. Jalalian *et al*., Computer-aided detection/diagnosis of breast cancer in mammography and ultrasound: A review, *Clinical Imaging* **37**(3) (2013) 420–426.
26. V. Bhateja, M. Misra and S. Urooj, Human visual system based unsharp masking for enhancement of mammographic images, *Journal of Computational Science* **21** (2017) 387–393.
27. A. Baccouche *et al*., Breast lesions detection and classification via YOLO-based fusion models.
28. S. Lixin *et al*., Segmentation of breast masses using adaptive region growing, in *Ifost* (IEEE, 2013).
29. W. Zhu *et al*., Adversarial deep structured nets for mass segmentation from mammograms, in *2018 IEEE 15th Int. Symp. on Biomedical Imaging* (*ISBI 2018*) (IEEE, 2018).
30. N. Dhungel, G. Carneiro and A. P. Bradley, Deep learning and structured prediction for the segmentation of mass in mammograms, in *Int. Conf. on Medical Image Computing and Computer-assisted Intervention* (Springer, 2015).
31. N. Dhungel, G. Carneiro and A. P. Bradley, Deep structured learning for mass segmentation from mammograms, in *2015 IEEE Int. Conf. on Image Processing* (*ICIP*) (IEEE, 2015).
32. N. Dhungel, G. Carneiro and A. P. Bradley, A deep learning approach for the analysis of masses in mammograms with minimal user intervention, *Medical Image Analysis* **37** (2017) 114–128.
33. H. Jung *et al*., Detection of masses in mammograms using a one-stage object detector based on a deep convolutional neural network, *PloS One* **13**(9) (2018) e0203355.

34. N. Dhungel, G. Carneiro and A. P. Bradley, Automated mass detection in mammograms using cascaded deep learning and random forests, in *2015 Int. Conf. on Digital Image Computing: Techniques and Applications* (*DICTA*) (IEEE, 2015).
35. J. Long, E. Shelhamer and T. Darrell, Fully convolutional networks for semantic segmentation, in *Proc. of the IEEE Conf. on Computer Vision and Pattern Recognition* (2015).
36. S. Li *et al*., Attention dense-U-Net for automatic breast mass segmentation in digital mammogram, *IEEE Access* **7** (2019) 59037–59047.
37. C. L. Chowdhary *et al*., An efficient segmentation and classification system in medical images using intuitionist possibilistic fuzzy C-mean clustering and fuzzy SVM algorithm, *Sensors* **20**(14) (2020) 3903.
38. Z. Hu *et al*., Deep learning for image-based cancer detection and diagnosis — A survey, *Pattern Recognition* **83** (2018) 134–149.
39. D. Abdelhafiz *et al*., Survey on deep convolutional neural networks in mammography, in *2017 IEEE 7th Int. Conf. on Computational Advances in Bio and Medical Sciences* (*ICCABS*) (IEEE, 2017).
40. D. Abdelhafiz *et al*., Deep convolutional neural networks for mammography: Advances, challenges and applications, *BMC Bioinformatics* **20**(11) (2019) 1–20.
41. G. Litjens *et al*., A survey on deep learning in medical image analysis, *Medical Image Analysis* **42** (2017) 60–88.
42. T. Shen *et al*., Simultaneous segmentation and classification of mass region from mammograms using a mixed-supervision guided deep model, *IEEE Signal Processing Letters* **27** (2019) 196–200.
43. A. Baccouche *et al*., Connected-UNets: A deep learning architecture for breast mass segmentation, *NPJ Breast Cancer* **7**(1) (2021) 1–12.
44. N. R. Rajalakshmi *et al*., Deeply supervised U-Net for mass segmentation in digital mammograms, *International Journal of Imaging Systems and Technology* **31**(1) (2021) 59–71.
45. D. Abdelhafiz *et al*., Residual deep learning system for mass segmentation and classification in mammography, in *Proc of the 10th ACM Int. Conf. on Bioinformatics, Computational Biology and Health Informatics* (2019).
46. R. Girshick *et al*., Rich feature hierarchies for accurate object detection and semantic segmentation, in *Proc. of the IEEE Conf. on Computer Vision and Pattern Recognition* (2014).
47. R. Girshick, Fast R-CNN, in *Proc. of the IEEE Int. Conf. on Computer Vision* (2015).
48. S. Ren *et al*., Faster R-CNN: Towards real-time object detection with region proposal networks, *Advances in Neural Information Processing Systems* **28** (2015) 91–99.
49. M. A. Al-Masni *et al*., Simultaneous detection and classification of breast masses in digital mammograms via a deep learning YOLO-based CAD system, *Computer Methods and Programs in Biomedicine* **157** (2018) 85–94.
50. E. Castro, J. S. Cardoso and J. C. Pereira, Elastic deformations for data augmentation in breast cancer mass detection, in *2018 IEEE EMBS Int. Conf. on Biomedical & Health Informatics* (*BHI*) (IEEE, 2018).
51. K. B. Soulami *et al*., Breast cancer: One-stage automated detection, segmentation, and classification of digital mammograms using UNet model based-semantic segmentation, *Biomedical Signal Processing and Control* **66** (2021) 102481.
52. L. Tsochatzidis *et al*., Integrating segmentation information into CNN for breast cancer diagnosis of mammographic masses, *Computer Methods and Programs in Biomedicine* **200** (2021) 105913.
53. V. K. Singh *et al*., Breast tumor segmentation and shape classification in mammograms using generative adversarial and convolutional neural network, *Expert Systems with Applications* **139** (2020) 112855.

54. D. Ribli *et al*., Detecting and classifying lesions in mammograms with deep learning, *Scientific Reports* **8**(1) (2018) 1–7.
55. S. Zahoor, U. Shoaib and I. U. Lali, Breast cancer mammograms classification using deep neural network and entropy-controlled whale optimization algorithm, *Diagnostics* **12**(2) (2022) 557.
56. Y. Wang *et al*., Whole mammographic mass segmentation using attention mechanism and multiscale pooling adversarial network, *Journal of Medical Imaging* **7**(5) (2020) 054503.
57. N. Dhungel, G. Carneiro and A. P. Bradley, Tree re-weighted belief propagation using deep learning potentials for mass segmentation from mammograms. in *2015 IEEE 12th Int. Symp. on Biomedical Imaging* (*ISBI*) (IEEE, 2015).
58. I. A. Lbachir, I. Daoudi and S. Tallal, Automatic computer-aided diagnosis system for mass detection and classification in mammography, *Multimedia Tools and Applications* **80**(6) (2021) 9493–9525.
59. R. Agarwal *et al*., Automatic mass detection in mammograms using deep convolutional neural networks, *Journal of Medical Imaging* **6**(3) (2019) 031409.
60. K. Zuiderveld, Contrast limited adaptive histogram equalization, *Graphics Gems* (1994) 474–485.
61. G. Deng, A generalized unsharp masking algorithm, *IEEE Transactions on Image Processing* **20**(5) (2010) 1249–1261.
62. J. Schmidhuber, Deep learning in neural networks: An overview, *Neural Networks* **61 (**2015) 85–117.
63. F. Yu and V. Koltun, Multi-scale context aggregation by dilated convolutions, arXiv preprint arXiv:1511.07122 (2015).
64. F. J. Ordóñez and D. Roggen, Deep convolutional and LSTM recurrent neural networks for multimodal wearable activity recognition, *Sensors* **16**(1) (2016) 115.
65. S.-H. Tsang, Review: DilatedNet-dilated convolution (semantic segmentation) (2018), Recuperado de: https://towardsdatascience. com/review-dilated-convolutionsemantic-segmentation-9d5a5bd768f5.
66. K. P. Murphy, *Machine Learning: A Probabilistic Perspective* (MIT Press, 2012).
67. Y. LeCun *et al*., Gradient-based learning applied to document recognition, in *Proc. of the IEEE* **86**(11) (1998) 2278–2324.
68. T. Sugino *et al*., Loss weightings for improving imbalanced brain structure segmentation using fully convolutional networks, in *Healthcare* (2021).
69. S. Ioffe and C. Szegedy, Batch normalization: Accelerating deep network training by reducing internal covariate shift, in *Int. Conf. on Machine Learning* (2015).
70. V. Nair and G. E. Hinton, Rectified linear units improve restricted Boltzmann machines, in *ICML* (2010).
71. Y. Lin and J. Wu, A novel multichannel dilated convolution neural network for human activity recognition, *Mathematical Problems in Engineering* **2020** (2020).
72. J. Chen *et al*., A novel multi-scale adversarial networks for precise segmentation of X-ray breast mass, *IEEE Access* **8** (2020) 103772–103781.
73. W. Zhao *et al*., Adaptive channel and multiscale spatial context network for breast mass segmentation in full-field mammograms, *Applied Intelligence* (2021) 1–18.